

# Simultaneous wavelength translation and amplitude modulation of single photons from a quantum dot

Matthew T. Rakher,<sup>1,\*</sup> Lijun Ma,<sup>2</sup> Marcelo Davanço,<sup>1,3</sup> Oliver Slattery,<sup>2</sup> Xiao Tang,<sup>2</sup> and Kartik Srinivasan<sup>1</sup>

<sup>1</sup>Center for Nanoscale Science and Technology, National Institute of Standards and Technology, Gaithersburg, MD 20899, USA

<sup>2</sup>Information Technology Laboratory, National Institute of Standards and Technology, Gaithersburg, MD 20899, USA

<sup>3</sup>Maryland NanoCenter, University of Maryland, College Park, MD 20742, USA

(Dated: October 18, 2018)

Hybrid quantum information devices that combine disparate physical systems interacting through photons offer the promise of combining low-loss telecommunications wavelength transmission with high fidelity visible wavelength storage and manipulation. The realization of such systems requires control over the waveform of single photons to achieve spectral and temporal matching. Here, we experimentally demonstrate the simultaneous wavelength conversion and temporal shaping of single photons generated by a quantum dot emitting near 1300 nm with an exponentially-decaying waveform (lifetime  $\approx 1.5$  ns). Quasi-phase-matched sum-frequency generation with a pulsed 1550 nm laser creates single photons at 710 nm with a controlled amplitude modulation at 350 ps timescales.

The integration of disparate quantum systems is an ongoing effort in the development of distributed quantum networks [1]. Two challenges in hybrid schemes which use photons for coupling include the differences in transition frequencies and linewidths among the component systems. Previous experiments using non-linear optical media to translate (or transduce) photons from one wavelength to another while preserving quantum-mechanical properties [2, 3] provide a means to overcome the first impediment. The second constraint has been addressed through single photon waveform manipulation using direct electro-optic modulation [4],  $\Lambda$ -type cavity-QED [5] and atomic ensemble systems [6], and conditional, non-local operations in spontaneous parametric downversion [7]. Here, we use pulsed frequency upconversion to simultaneously change the frequency and temporal amplitude profile of single photons produced by a semiconductor quantum dot (QD). Triggered single photons that have an exponentially decaying temporal profile with a time constant of 1.5 ns and a wavelength of 1300 nm are converted to photons that have a Gaussian temporal profile with a controllable full-width at half-maximum (FWHM) as narrow as  $350 \text{ ps} \pm 16 \text{ ps}$  and a wavelength of 710 nm. The use of a high conversion efficiency nonlinear waveguide and low-loss fiber optics results in a 16 % overall efficiency in producing such frequency converted, amplitude-modulated photons. The simultaneous combination of wavepacket manipulation and quantum frequency conversion may be valuable in integrating telecommunications-band semiconductor QDs with broadband visible wavelength quantum memories [8] as part of a distributed quantum network, for the creation of ultra-high bandwidth [9], indistinguishable photons from disparate quantum emitters, and for efficient, temporally-resolved photon counting at the ps level.

Single epitaxially-grown semiconductor QDs are promising stable, bright, and scalable on-demand sources of single photons [10], with improvements in photon

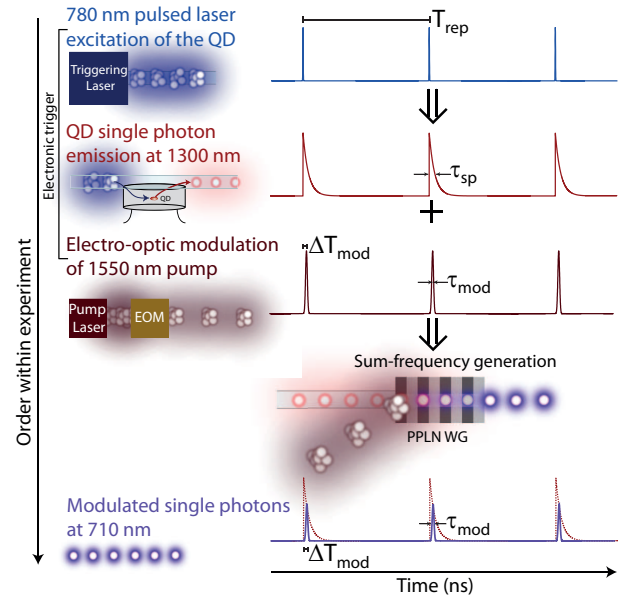


FIG. 1. Schematic of the experiment for simultaneous wavelength translation and amplitude modulation of single photons from a quantum dot.

extraction efficiency [11], suppression of multi-photon events [11, 12], and photon indistinguishability [12, 13] indicative of their potential for high performance in quantum information applications. On the other hand, the dominant and most mature system for such QD single photon source developments has been the InGaAs/GaAs material system, whose band structure constrains the range of available emission energies, and temporal control of the photon wavepacket shape remains a challenge in these systems. Despite recent progress [14], access to three-level Raman transitions in which the temporal shape is determined by the pump mode profile, a staple of trapped atom and ion systems [5, 15] is typically not available. Instead, most QDs are two-level systems in which the emitted photons have an exponentially decay-

ing temporal profile, and temporal shaping must occur after photon generation. As we describe below, the method used in this work produces wavelength-translated, single photon wavepackets with a temporal profile inherited from the classical pump beam used in the frequency up-conversion process. Though this technique is not lossless, it can still be quite efficient, is flexible, straightforward to use on existing devices, and operates on the nanosecond timescales requisite for QD experiments and for which classical coherent pulse shaping techniques [16] are difficult to implement. In comparison to direct amplitude modulation of single photon wavepackets [4], the technique presented here has lower loss, can operate on much faster timescales using existing mode-locked laser technologies, and importantly, simultaneously changes the wavelength of the photons. This is necessary for integration with visible wavelength quantum systems and provides a method to overcome spectral and temporal distinguishability of disparate quantum sources.

We generated single photons at  $1.3 \mu\text{m}$  from a single InAs QD embedded in a GaAs mesa [17]. The QD sample is cooled to a temperature of  $\approx 7 \text{ K}$ , excited with a repetitively pulsed (50 MHz) laser, and its photoluminescence (PL) is out-coupled into a single mode fiber as depicted in Fig. 1. The PL is directed either into a grating spectrometer for characterization or into the pulsed upconversion setup for simultaneous wavelength translation and amplitude modulation. The PL spectrum from a single QD measured by the spectrometer is shown in Fig. 2(a). It displays two sharp peaks corresponding to two excitonic charge configurations,  $X^+$  near 1296 nm, and  $X^0$  near 1297 nm. Photons emitted at the  $X^0$  transition wavelength will be used for the experiments described hereafter.

PL from the  $X^0$  transition is directed into an upconversion setup where it is combined with a strong 1550 nm pulse in a periodically-poled LiNbO<sub>3</sub> (PPLN) waveguide [17]. A simplified schematic of the experimental timing sequence is shown in Fig. 1. The pump pulse is created by gating the output of a tunable laser with an electro-optic modulator (EOM). An electrical pulse generator drives the EOM synchronously with the 780 nm QD excitation laser, but at half the repetition rate (25 MHz), using a trigger signal from the delay generator. These instruments combine to generate electrical pulses with controllable FWHM ( $\tau_{mod}$ ) and delay ( $\Delta T_{mod}$ ) as shown in Fig. 1, and the resulting optical pulses have an extinction ratio  $> 20 \text{ dB}$ . The modulated 1550 nm pump signal is amplified to produce a peak power of 85 mW entering the PPLN waveguide where it interacts with a 1300 nm QD single photon to create a single photon at the sum-frequency near 710 nm. This  $\chi^{(2)}$  process is made efficient through quasi-phase-matching by periodic poling [18] as well as the tight optical confinement of the waveguide [19]. Previous measurements using a continuous-wave (CW) pump in the same setup demon-

strated single-photon conversion efficiencies  $\gtrsim 75 \%$  [3], and others have measured efficiencies near unity with attenuated laser pulses [20, 21]. Light exiting the PPLN is spectrally filtered to isolate the 710 nm photons, which are detected by Si single photon counting avalanche detectors (SPADs) for excited state lifetime and second-order correlation measurement ( $g^{(2)}(\tau)$ ).

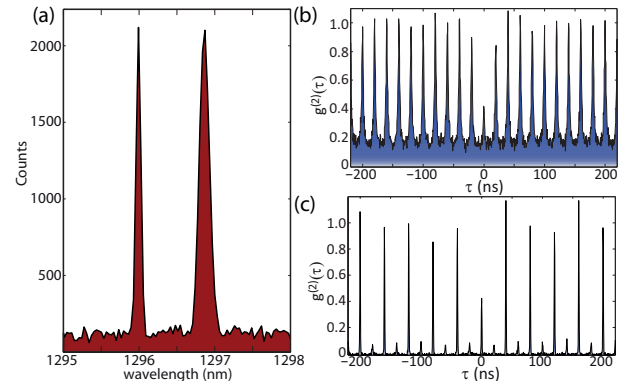


FIG. 2. (a) PL spectrum of a single QD after 60 s integration showing two excitonic transitions,  $X^+$  (1296 nm) and  $X^0$  (1297 nm). (b-c) Second-order intensity correlation,  $g^{(2)}(\tau)$ , of single photons upconverted with a CW pump, where  $g^{(2)}(0) = 0.41 \pm 0.02$  (c) and a pulsed pump with  $\tau_{mod} = 500$  ps, where  $g^{(2)}(0) = 0.45 \pm 0.03$  (d) for an integration time of 7200 s.

First, we compare the measured  $g^{(2)}(\tau)$  for photons that are upconverted using a 1550 nm CW pump (Fig. 2(b)) and 500 ps pulses (Fig. 2(c)) with the same peak power of 85 mW. Both are antibunched with  $g^{(2)}(0) < 0.5$ , showing that the signal is dominantly composed of single photons in both cases. However, pulsed pumping reduces events that are uncorrelated in time with the QD single photons and contribute a constant background. This unwanted background results from upconversion of anti-Stokes Raman photons from the strong (CW) 1550 nm beam [20], and is seen in Fig. 2(b) but not in Fig. 2(c). For understanding the origin of the non-zero  $g^{(2)}(0)$  value, the background is helpful in distinguishing the fraction due to anti-Stokes Raman photons from that due to upconversion of multi-photon emission from the QD sample [3]. For a practical implementation, however, it adds a constant level to the communications channel and pulsed upconversion removes this noise without gating of the detector. Ideally, Fig. 2(c) would only show peaks spaced by 40 ns, due to the 25 MHz repetition rate of the EOM. In practice, the small peaks spaced 20 ns from the large peaks are due to imperfect extinction of the EOM and pulse generator, resulting in upconversion of QD photons when the EOM is nominally off.

Next, we perform time-resolved measurements of the upconverted 710 nm photons. In recent work [3] using a CW 1550 nm pump beam, the temporal amplitude profile of the upconverted 710 nm photon exactly matched that

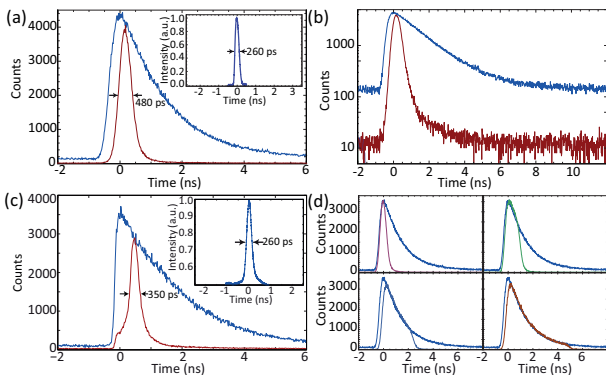


FIG. 3. (a,b) Temporal profile of the upconverted photons using a CW (blue) and  $\tau_{mod} = 260$  ps pulsed (maroon) 1550 nm pump on linear (a) and log (b) scales. Inset: 1550 nm pump pulse measured by the optical communications analyzer. (c) Same as (a) but using a reduced timing jitter SPAD. (d) Temporal profile of upconverted photons using  $\tau_{mod} = \{0.5, 1.25, 2.5, 5.1\}$  ns along with a CW pump. All measurements are taken with 1200 s integration.

of the original 1300 nm photon, and was used to measure the QD lifetime with dramatically better dynamic range than with a telecommunications SPAD. Here, the pulsed 1550 nm pump not only upconverts the QD photon to 710 nm, but also modulates its temporal amplitude profile because  $\tau_{mod}$  is less than the lifetime of the QD transition ( $\approx 1.5$  ns). Figure 3(a) displays the temporal amplitude profile of 710 nm single photons generated using a 1550 nm pulse with  $\tau_{mod} = 260$  ps (maroon), along with that of single photons generated with a CW pump (blue) for comparison. The measured  $480 \text{ ps} \pm 16 \text{ ps}$  FWHM of the upconverted photon is limited by the  $\approx 350$  ps timing jitter of the Si SPAD and its uncertainty is given by the timebase of the photon counting board. The same plot is reproduced in Fig. 3(b) on a log scale, with an apparent increase in the dynamic range due to the removal of CW anti-Stokes Raman photons. This same measurement was performed using a SPAD with a reduced timing jitter ( $\approx 50$  ps), and the resulting data is shown in Fig. 3(c) corresponding to a FWHM of  $350 \text{ ps} \pm 16 \text{ ps}$ . Here, the resulting FWHM is not limited by the detector timing jitter but by an effective broadening of the pump pulse in the frequency conversion process [17]. Even so, taken together with the commercial availability of 40 GHz EOMs and drivers for 1550 nm lasers, these results demonstrate a first step towards the creation of quantum light sources that are modulated to operate near the capacity of telecommunications channels [9]. To show the versatility of the setup, Fig. 3(d) shows the temporal profile of QD single photons after upconversion using pump pulse widths of  $\tau_{mod} = 500 \text{ ps}, 1.25 \text{ ns}, 2.5 \text{ ns},$  and  $5.1 \text{ ns}$  along with a CW pump for comparison. By simply adjusting the pulse generator that drives the EOM, one can create single photons of arbitrary width and shape [17].

In addition to changing  $\tau_{mod}$ , the delay between the arrival of the QD single photon and pump pulse,  $\Delta T_{mod}$ , can also be varied (Fig. 1). Figure 4(a)-(b) show the result of such a measurement in linear (a) and log (b) scale for  $\Delta T_{mod} = \{0.0, 0.5, 1.0, 1.5, 2.0, 2.5, 3.0, 3.35\}$  ns under pulsed pumping with  $\tau_{mod} = 260$  ps. The inset of (a) shows a similar measurement using the reduced timing jitter SPAD. The peaks heights nicely follow the decay curve of the CW profile, shown in blue for comparison. This measurement suggests that pulsed frequency upconversion could be used for achieving high timing resolution in experiments on single quantum emitters. These time-correlated single photon counting experiments are currently limited by the timing jitter of the SPAD, which is typically  $> 50$  ps. The time-domain sampling enabled by pulsed upconversion [22] provides a timing resolution set by  $\tau_{mod}$ , which is limited by the quasi-phase-matching spectral bandwidth of the non-linear material. For the PPLN waveguide used here, the bandwidth ( $\approx 0.35$  nm) corresponds to a minimum  $\tau_{mod} \approx 10$  ps, while sub-ps timing resolution should be available in broader bandwidth systems [23]. Sub-ps 1550 nm pulses can be generated by mode-locked fiber lasers, and if applied as in Fig. 4(a)-(b), could trace out emission dynamics with a timing resolution 1-2 orders of magnitude better than the typical timing jitter of a SPAD, allowing, for example, measurement of beat phenomena within the QD [24] or time-domain observation of vacuum Rabi oscillations in cavity quantum electrodynamics [25].

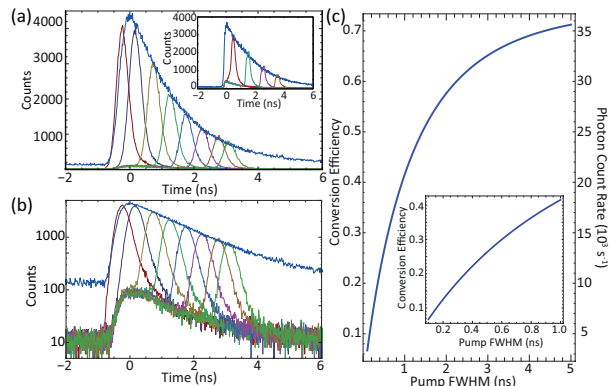


FIG. 4. (a,b) Temporal profile of the upconverted photons using a CW (blue) and  $\tau_{mod} = 260$  ps pulsed (various colors) 1550 nm pump on linear (a) and log (b) scales for delays  $\Delta T_{mod} = \{0.0, 0.5, 1.0, 1.5, 2.0, 2.5, 3.0, 3.35\}$  ns. Inset: Similar measurement as (a), but measured with reduced timing jitter SPAD. All measurements are taken with 1200 s integration. (c) Net conversion efficiency and photon count rate as a function of the pump pulse FWHM,  $\tau_{mod}$ . Inset: Focus on sub-ns regime.

The data from Figs. 2 and 3 indicate that while the quantum nature of the photon has been inherited from the QD emission near 1300 nm, its temporal profile has been inherited from the strong pump pulse near 1550 nm.

This is a direct consequence of the nonlinear nature of the upconversion process. However, because QD-generated single photons have a coherence time that is typically less than twice the lifetime, they are not perfectly indistinguishable [13]. This arises due to interaction of the confined carriers in the QD with the surrounding crystal and, for the type of QD considered here, yields a coherence time of  $\approx 280$  ps [25] and an indistinguishability of  $\approx 10$  %. For our experiments, this means that each photon is not modulated in the same way and the resulting histograms are ensemble averages. Nonetheless, the experiments would proceed in the exact same manner for more ideal photons, such as those produced with a ns coherence time through near-resonant excitation [12]. In fact, simultaneous frequency translation and amplitude modulation can be used to generate indistinguishable single photons from non-identical QDs [26]. Frequency translation can move each single photon to the same wavelength while amplitude modulation can be used to select the coherent part of the wave-packet. Since the quasi-phase-matching of the PPLN can be tuned by temperature, this offers the ability to create indistinguishable single photons from QDs spectrally separated by the entire inhomogeneous linewidth of the QD distribution (which is usually tens of nanometers) without the need for electrical gates or modification of the sample.

The single photon manipulation demonstrated here is essentially a combination of quantum frequency conversion and amplitude modulation. Coherent pulse-shaping techniques [16], which have been used with entangled photon pairs [27], are currently quite difficult to directly apply to QD single photons due to their narrow spectral bandwidth compared to photons produced by parametric downconversion, for example. Furthermore, recent work [9] has suggested that a combination of frequency upconversion using a spectrally tailored 1550 nm pump beam and spectral phase correction may be an approach to lossless shaping of QD single photons. Our work, utilizing a similar sum frequency generation approach, represents a step towards such a goal. Though our approach is not lossless, broadband insertion loss (usually  $> 3$  dB) is avoided in comparison to direct amplitude modulation of the single photon state because the modulation in nonlinear mixing approaches such as ours and that of Ref. [9] is performed on the classical pump beam. Nonetheless, the fact that the pump pulse is temporally shorter than the single photon wave-packet introduces extra loss. A full derivation of this loss is included in the supplemental material [17], but the result is shown in Fig. 4(c) which plots the net conversion efficiency as a function of the pump pulse FWHM,  $\tau_{mod}$ , from 100 ps to 5 ns (inset displays sub-ns regime). The efficiency asymptotically approaches 75 %, the measured conversion efficiency with a CW pump, and ranges from 16 % for  $\tau_{mod} = 260$  ps to 71 % for  $\tau_{mod} = 5$  ns. For our FTW-based PL collection with 0.1 % collection efficiency and 50 MHz exci-

tation rate, this translates to a single photon count rate of  $8000\text{ s}^{-1}$  to  $36000\text{ s}^{-1}$  as shown on the right axis in Fig. 4(c). Using more advanced techniques that have demonstrated  $>10$  % collection efficiency [11], the overall production rate of frequency translated, temporally modulated single photons can easily reach  $10^6\text{ s}^{-1}$ .

In summary, we have demonstrated simultaneous wavelength translation and amplitude modulation of a single photon from a quantum dot using pulsed frequency upconversion. The use of a quasi-phase-matched waveguide and low-loss fiber optics results in a 16 % overall conversion efficiency in producing Gaussian-shaped, single photon pulses near 710 nm with a FWHM of 350 ps from single photons near  $1.3\text{ }\mu\text{m}$  with an exponentially-decaying wavepacket. Such methods may prove valuable for integrating disparate quantum systems, creating ultra-high bandwidth indistinguishable single photon sources, and for achieving high resolution in time-resolved experiments of single quantum systems.

---

\* matthew.rakher@gmail.com; Current Address: Departement Physik, Universität Basel, Klingelbergstrasse 82, CH-4056 Basel, Switzerland

- [1] H. J. Kimble, *Nature (London)* **453**, 1023 (2008).
- [2] J. M. Huang and P. Kumar, *Phys. Rev. Lett.* **68**, 2153 (1992); S. Tanzilli *et al.*, *Nature* **437**, 116 (2005); H. J. McGuinness *et al.*, *Phys. Rev. Lett.* **105**, 093604 (2010).
- [3] M. T. Rakher *et al.*, *Nature Photonics* **4**, 786 (2010).
- [4] P. Kolchin *et al.*, *Phys. Rev. Lett.* **101**, 103601 (2008); H. P. Specht *et al.*, *Nature Photonics* **3**, 469 (2009); M. T. Rakher and K. Srinivasan, *Appl. Phys. Lett.* **98**, 211103 (2011).
- [5] J. McKeever *et al.*, *Science* **303**, 1992 (2004); M. Keller *et al.*, *Nature* **431**, 1075 (2004).
- [6] M. D. Eisaman *et al.*, *Phys. Rev. Lett.* **93**, 233602 (2004); J. F. Chen *et al.*, *Phys. Rev. Lett.* **104**, 183604 (2010).
- [7] S.-Y. Baek, O. Kwon, and Y.-H. Kim, *Phys. Rev. A* **77**, 013829 (2008).
- [8] K. F. Reim *et al.*, *Nature Photonics* **4**, 218 (2010); E. Saglamyurek *et al.*, *Nature (London)* **469**, 512 (2011).
- [9] D. Kielpinski, J. F. Corney, and H. M. Wiseman, *Phys. Rev. Lett.* **106**, 130501 (2011).
- [10] A. J. Shields, *Nature Photonics* **1**, 215 (2007).
- [11] S. Strauf *et al.*, *Nature Photonics* **1**, 704 (2007); J. Claudon *et al.*, *Nature Photonics* **4**, 174 (2010).
- [12] S. Ates *et al.*, *Phys. Rev. Lett.* **103**, 167402 (2009).
- [13] C. Santori *et al.*, *Nature* **419**, 594 (2002).
- [14] G. Fernandez *et al.*, *Phys. Rev. Lett.* **103**, 087406 (2009).
- [15] G. S. Vasilev, D. Ljunggren, and A. Kuhn, *New Journal of Physics* **12**, 063024 (2010).
- [16] A. M. Weiner, *Review of Scientific Instruments* **71**, 1929 (2000).
- [17] See Supplemental Material at [URL will be inserted by publisher] for experimental details, a full analysis of the total conversion efficiency, and more complex amplitude profiles.
- [18] M. M. Fejer *et al.*, *IEEE J. Quan. Elec.* **28**, 2631 (1992).

- [19] L. Chanvillard *et al.*, Appl. Phys. Lett. **76**, 1089 (2000).
- [20] C. Langrock *et al.*, Opt. Lett. **30**, 1725 (2005).
- [21] A. Vandevender and P. Kwiat, J. Mod. Opt. **51**, 1433 (2004); M. Albota and F. Wong, Opt. Lett. **29**, 1449 (2004); H. Xu *et al.*, Opt. Express **15**, 7247 (2007).
- [22] J. Shah, IEEE J. Quan. Elec. **24**, 276 (1988); L. Ma, J. C. Bienfang, O. Slattery, and X. Tang, Opt. Express **19**, 5470 (2011).
- [23] O. Kuzucu *et al.*, Opt. Lett. **33**, 2257 (2008); H. Suchowski *et al.*, Opt. Photon. News **21**, 36 (2010).
- [24] T. Flissikowski *et al.*, Phys. Rev. Lett. **86**, 3172 (2001).
- [25] K. Srinivasan *et al.*, Phys. Rev. A **78**, 033839 (2008).
- [26] R. B. Patel *et al.*, Nature Photonics **4**, 632 (2010); E. B. Flagg *et al.*, Phys. Rev. Lett. **104**, 137401 (2010).
- [27] A. Pe'er *et al.*, Phys. Rev. Lett. **94**, 073601 (2005).